

Physio-mechanical properties of an active chitosan film incorporated with montmorillonite and natural antioxidants extracted from pomegranate rind

Yu-Yue Qin · Zhi-Hong Zhang · Lin Li ·
Ming-Long Yuan · Jian Fan · Tian-Rui Zhao

Revised: 22 July 2013 / Accepted: 1 August 2013 / Published online: 14 August 2013
© Association of Food Scientists & Technologists (India) 2013

Abstract An active film was prepared from chitosan incorporated with montmorillonite (MMT) and pomegranate rind powder extract (PRP). The effect of MMT (1 %, 3 %, and 5 % w/w chitosan) and PRP (1 %, 1.5 %, and 2 % w/v chitosan) on the physical, mechanical and antioxidant properties of the chitosan-based films was studied. Fourier transform infrared (FTIR) spectra revealed that good interactions occurred between functional groups of chitosan with MMT or with PRP. The results showed that the water vapor barrier property of the films was significantly improved by incorporation of MMT and PRP ($p < 0.05$). When compared to pure chitosan film, the WVP of M3P2 film (Chitosan/3 % MMT/2 % PRP) decreased by 25.2 %. Tensile strength of the films was affected by the addition of MMT and PRP. However, percent elongation at break was not significantly changed by addition of PRP. The film incorporated with 3 % MMT and 2 % PRP that contained the highest amount of total phenolic (15.2 mg GAE/g DW), was found to be the most active radical scavenger. These results suggest that chitosan films containing MMT and PRP can be used for development of active food packaging materials.

Keywords Chitosan · Composite film · Montmorillonite · Pomegranate rind powder extract · Active food packaging · Physio-mechanical properties

Introduction

Over the last two decades, considerable research has been conducted to develop and apply biopolymers. Chitosan is a natural carbohydrate polymer obtained by the deacetylation of chitin, and chitin is a major component of shells of crustaceans such as crab, shrimp and crawfish (Vásconez et al. 2009; Guldás et al. 2010; Gómez-Estaca et al. 2011). It has immense potential as a packaging material owing to non-toxicity, biodegradability, biocompatibility and antimicrobial activity (Mathew and Abraham 2008; Harris et al. 2011). However, the shortcoming of pure chitosan limits its application because it causes the resulting film to exhibit a low water vapor barrier and poor mechanical properties.

Recently, the application of nanocomposite technology has proven to be a promising option. The addition of montmorillonite (MMT) could effectively improve mechanical properties and decrease the water vapor permeability of chitosan film (Rhim 2006; Abdollahi et al. 2012). If the MMT loading level is 1–5 % (w/w), the clay particles can be properly dispersed in the polymer matrix, and unique combinations of physical and chemical properties of chitosan-based films will be obtained (Casariego et al. 2009). In addition, montmorillonite has been successfully applied in food packaging (Hu et al. 2011; Avella et al. 2005; Costa et al. 2011).

Active compounds, such as antioxidants, antibacterial agents, flavors and nutrients, can be incorporated into packaging materials in order to provide several functions that do not exist in conventional packaging systems (Jamshidian et al. 2012; Kanatt et al. 2012). Due to reports of possible toxic

Y.-Y. Qin (✉) · Z.-H. Zhang · J. Fan · T.-R. Zhao
Research Centre of Food Engineering, Kunming University of
Science and Technology, Kunming, Yunnan, China 650550
e-mail: rabbqy@163.com

L. Li
College of Light Industry and Food Science, South China University
of Technology, Guangzhou, Guangdong, China 510640

M.-L. Yuan
School of Chemistry and Biotechnology, Yunnan University of
Nationalities, Kunming, Yunnan, China 650504

effects from synthetic antioxidants, the interest for alternative methods to retard lipid oxidation in foods, such as the use of natural antioxidants, has increased (Selani et al. 2011). However, natural extracts are often more expensive and less effective than synthetic antioxidants (Huang et al. 2011). As a result, special attention has been focused on those from inexpensive or residual sources from agriculture industries.

Pomegranate (*Punica granatum* L.) rind is by-products obtained during processing of pomegranate juice. Pomegranate rind powder extract (PRP) is proved to exhibit good antioxidant activity due to polyphenolic compounds such as ellagic tannins, ellagic acid and gallic acid (Negi et al. 2003). PRP has been reported to delay the onset lipid oxidation in various meat and meat products including raw chicken patties (Devatkal et al. 2011), cooked chicken patties (Naveena et al. 2008) and goat meat (Devatkal and Naveena 2010).

The aim of the study was to develop composite films from chitosan incorporated with montmorillonite (MMT) and pomegranate rind powder extract (PRP). Film thickness, water vapor permeability, mechanical property, optical property, total phenolic content, and antioxidant activity were also investigated.

Materials and methods

Acetic acid was obtained from Beijing Chemical Works (Beijing, China), chitosan from Qingdao Allforlong Bio-tech Co., Ltd. (Shandong, China), and montmorillonite (MMT) from Fenghong Clay Chemical Co., Ltd. (Zhejiang Province, China). 2,2-Diphenyl-1-picrylhydrazyl (DPPH), rutin, gallic acid were obtained from Sigma Chemical Inc., USA. Forint phenol reagent was obtained from Shanghai Hualan Chemical Technology Co., Ltd, China. Agar powder, yeast extract and peptone were purchased from Aoboxing Bio-tech Co., Ltd (Beijing, China). All other reagents and chemicals used were of analytical grade procured from local sources.

Preparation of Pomegranate Rind Powder extract (PRP) Mature and healthy pomegranate fruits were collected from Yunnan Province, China. Fruits were washed, cut manually and peeled off. Then, pomegranate peels were dried in an air circulatory tray drier at 60 °C for 48 h. Dried peels were powdered using a mixer grinder. 10 g of dried pomegranate powder was extracted with 80 % ethanol (200 ml) overnight at 40 °C in a shaking water bath. The supernatant was filtered through a filter paper and concentrated using a rotary evaporator below 50 °C. After evaporation of ethanol, pomegranate rind powder extract was freeze-dried and stored at 4 °C until use.

Preparation of chitosan/MMT-PRP solutions Aqueous solution was prepared according to the method established by Rhim et al. (2006). For pure chitosan film, chitosan powder was dissolved in a constantly stirred (800 rpm) 2 % (v/v)

acetic acid aqueous solution for 6 h to a final concentration of 1.5 % (w/v). For chitosan/MMT film, 1 %, 3 % and 5 % of montmorillonite (w/w, relative to chitosan on a dry basis) was dispersed in a 2 % acetic acid solution by vigorous mixing (800 rpm) for 1 h to obtain a montmorillonite solution. Then, pure chitosan solution was added to montmorillonite solution by vigorous mixing (800 rpm) at 60 °C. For chitosan/MMT-PRP film, 1 %, 1.5 % and 2 % of PRP (w/v relative to neat chitosan solution) was added to chitosan/MMT solution by homogenizing at 7,000 rpm for 2 min. Glycerol (0.1 % v/v of film-forming solution) was employed as the plasticizer in all the films. After cooling the resulting solution at room temperature, it was degassed under vacuum for 10 min in order to remove all bubbles. The compositions of chitosan-based films were listed in Table 1.

Film preparation The solutions were filtered and cast onto a polytetrafluoroethylene (PTFE) plate for the preparation of film. All of the films were dried in an oven at 40 °C and cut into 10 cm×2.54 cm. Dried films were stored in a desiccator containing saturated magnesium nitrate solution at 25 °C and 50 % relative humidity until evaluation.

Sample characterization

Fourier Transform Infrared (FTIR) analysis Spectrometry was carried out to observe the structural interactions of chitosan films incorporated with MMT and PRP. FTIR spectra were collected in the range of 400–4,000 cm^{-1} at resolution of 4 cm^{-1} using an FTIR spectrometer (Nicolet iS10, Madison, USA). All the readings were performed at room temperature (20 °C).

Film thickness measurements Film thickness was measured using a digital micrometer (Mitotuyo No. 7327, Tokyo, Japan). Five replications were conducted for each sample treatment. Measurements were taken at five different locations of each film sample and the mean values were calculated.

Scanning Electron Microscopy (SEM) SEM was used to examine the surface morphology of chitosan-based films. The films were first sputter-coated with a thin conductive gold layer and then the morphology was studied using Hitachi S-4800 (Japan).

Water Vapor Permeability (WVP) The water vapor permeability of films was determined according to the method of Vásconez et al. (2009) with some modifications. The test acrylic cups had diameter of 40 mm and were 25 mm deep. They contained desiccant (silica gel) to generate a 0 % RH inside the cell and were sealed with the test film previously equilibrated at 25 °C and 50 % RH for 2 h. Then, the covered

Table 1 Water vapor permeability and mechanical properties of chitosan-based films

Film	Concentration		Thickness (μm)	WVP ($\times 10^{-9} \text{ g} \cdot \text{m}/\text{m}^2 \cdot \text{s} \cdot \text{Pa}$)	TS (MPa)	E (%)
	MMT (%w/w chitosan)	PRP (%w/v chitosan solution)				
Control	Control		65.0 \pm 2.3 ^a	2.18 \pm 0.02 ^f	20.8 \pm 1.2 ^a	12.7 \pm 0.8 ^a
M1	1	0	69.5 \pm 5.8 ^{ab}	1.93 \pm 0.03 ^e	26.3 \pm 2.3 ^b	15.9 \pm 1.3 ^b
M1P1	1	1	71.2 \pm 6.5 ^{abc}	1.83 \pm 0.02 ^{cde}	29.5 \pm 1.8 ^{bc}	15.2 \pm 0.8 ^b
M1P1.5	1	1.5	72.6 \pm 2.3 ^{bc}	1.77 \pm 0.01 ^{cd}	34.6 \pm 2.1 ^{de}	15.8 \pm 2.2 ^b
M1P2	1	2	84.0 \pm 1.0 ^{ef}	1.71 \pm 0.02 ^{bc}	35.0 \pm 0.8 ^{de}	14.9 \pm 0.7 ^b
M3	3	0	74.6 \pm 2.7 ^{bc}	1.88 \pm 0.01 ^{de}	33.4 \pm 4.9 ^{cd}	17.0 \pm 1.8 ^b
M3P1	3	1	75.2 \pm 3.5 ^{bcd}	1.81 \pm 0.02 ^{cd}	36.8 \pm 3.6 ^e	16.3 \pm 2.1 ^b
M3P1.5	3	1.5	82.4 \pm 1.2 ^{def}	1.72 \pm 0.01 ^{bc}	40.6 \pm 3.5 ^{fg}	17.4 \pm 1.3 ^b
M3P2	3	2	86.6 \pm 1.6 ^f	1.63 \pm 0.02 ^b	42.7 \pm 2.0 ^h	16.9 \pm 0.3 ^b
M5	5	0	74.8 \pm 7.1 ^{bc}	1.73 \pm 0.15 ^{bc}	32.3 \pm 3.3 ^{cd}	16.7 \pm 0.6 ^b
M5P1	5	1	76.2 \pm 1.1 ^{bcd}	1.63 \pm 0.07 ^b	37.1 \pm 0.4 ^{ef}	17.2 \pm 1.1 ^b
M5P1.5	5	1.5	78.2 \pm 3.9 ^{cde}	1.46 \pm 0.04 ^a	39.4 \pm 4.7 ^{fg}	16.5 \pm 1.5 ^b
M5P2	5	2	85.0 \pm 5.9 ^{ef}	1.47 \pm 0.15 ^a	40.9 \pm 4.5 ^g	16.6 \pm 0.4 ^b

*Values are given as mean \pm standard deviation. Values followed by different letters in the same row are significantly different ($p < 0.05$), a =the lowest value

cups were placed in a temperature and RH controlled chamber with the same conditions required for film equilibration. The weight loss of the cup was considered equal with the transferred water through the film and adsorbed by the desiccant. Changes in the weight of the cup were recorded at intervals of 2 h for 12 h and were plotted as a function of time. The water vapor permeability of the film was calculated using the following equation (Martins et al. 2012).

$$WVP = (WVTR \times L) / \Delta P \tag{1}$$

where $WVTR$ is the water vapor transmission rate ($\text{g}/\text{m}^2 \cdot \text{s}$) through the film, L is the average film thickness (m), and ΔP is the partial water vapor pressure difference (Pa) between the two sides of the film. This test was replicated three times for each sample.

Mechanical properties The tensile strength (TS) and elongation at break (E) of samples were determined with a Universal tensile machine (WDW-10, Shanghai Jadaronsen M&C System Co., Ltd., Shanghai, China). The initial grip separation was set at 50 mm and the crosshead speed was set at 100 mm/min (Seog et al. 2008). The mechanical test was carried out at room temperature and replicated five times for each sample.

Opacity measurement Opacity was determined according to the method of Park et al. (2004). Absorption at 600 nm was measured using a UV–vis spectrophotometer (T90, Beijing Purkinje general instrument Co., Ltd. Beijing, China). Each film sample was cut into a rectangle piece (0.7 cm \times 1.5 cm

and directly placed in a spectrophotometer test cell. An empty test cell was used as the reference. The opacity of the films was calculated by the following equation.

$$T = \frac{Abs_{600}}{d} \tag{2}$$

where T is the transparency, Abs_{600} is the value of absorbance at 600 nm and d is the film thickness (mm). According to this equation, the high values of T indicate lower transparency and higher degree of opacity (Siripatrawan and Harte 2010).

Total Phenolic Content (TPC) For this purpose, 50 mg of each film sample was dissolved in 5 ml of methanol. Total phenolic content (TPC) of film samples was determined according to the Folin-Ciocalteu assay (Moradi et al. 2012). Aliquots of 0.5 ml film extracts were mixed with 2.5 ml of Forint phenol reagent and 2 ml of 7.5 % NaHCO_3 . The tube was allowed to stand for 60 min at room temperature. Absorption at 765 nm was measured using a UV–vis spectrophotometer. The total phenolic content was expressed as gallic acid equivalents (mg GAE/g DW), and the values are presented as means of triplicate analyses.

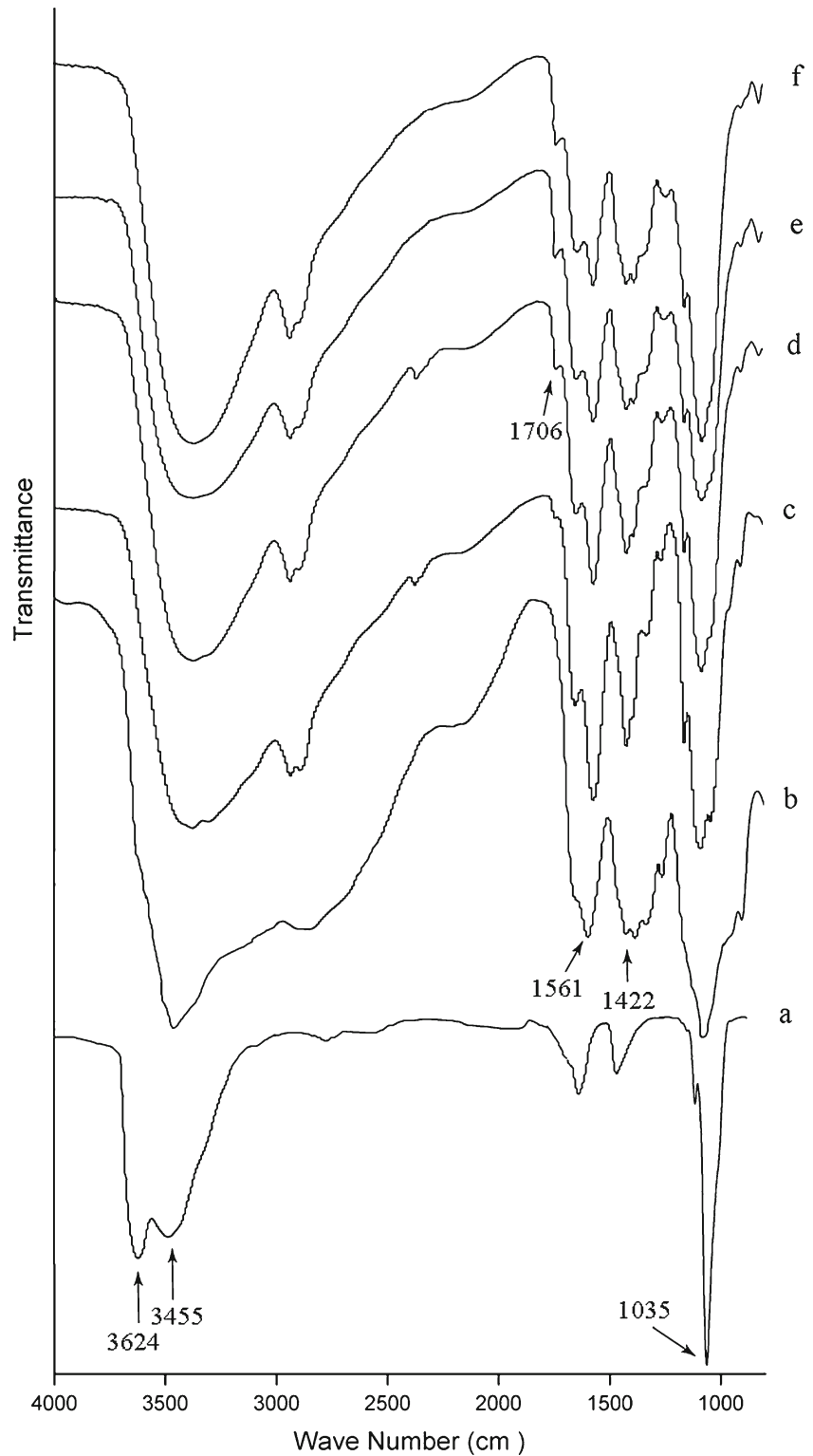
DPPH radical-scavenging ability The 1,1-diphenyl-2-picrylhydrazyl (DPPH) free radical-scavenging ability assay was performed according to the method of Takao et al. (1994) and Kumarasamy et al. (2007) with slight modifications. 4 mg of DPPH was dissolved in 100 ml of MeOH to obtain a concentration of 0.1 mmol/ml. 2 ml of film extract solution was then

mixed with 2 ml of DPPH solution. The samples were kept in the dark for 30 min at room temperature. Spectrophotometric measurement was made using methanol as blank and absorption was measured at 517 nm. Blank sample and DPPH solution were prepared and measured daily. The percent

inhibition of the DPPH radical was calculated by the following formula:

$$\text{Inhibition percentage(\%)} = (1 - A_s/A_c) \times 100 \quad (3)$$

Fig. 1 FTIR spectra of **a** MMT, **b** pure chitosan, **c** M3, **d** M3P1, **e** M3P1.5, and **f** M3P2. M3, M3P1, M3P1.5, and M3P2—see Table 1



Where

A_S absorption of film extract solution;

A_C absorption of blank sample.

Statistical analysis SPSS statistical computer software package (SPSS version 13.0) was employed in this study. Analysis of variance (ANOVA) was performed on all observed data. Experimental data were the mean \pm SD of three replicates of the determinations for each sample. Duncan's multiple comparison test were performed to determine the difference of means, and $p < 0.05$ was considered to be statistically significant.

Results and discussion

FTIR spectra analysis FTIR spectra were used to identify possible interactions between functional groups of chitosan with MMT or with PRP. Figure 1 showed the spectra of chitosan, MMT, chitosan/MMT blend films and chitosan/MMT-PRP blend films. It is reported that when two or more substances are mixed, physical blends versus chemical interactions are reflected by changes in characteristic spectra peaks (Xu et al. 2005).

The spectrum of MMT (Fig. 1a) showed the characteristic bands $3,624\text{ cm}^{-1}$ due to O-H stretching, a broad peak centred on $3,455\text{ cm}^{-1}$ due to interlayer and intralayer H-bonded O-H stretching. The peak at $1,637\text{ cm}^{-1}$ was the H-O-H bending vibrations. The sharp peak at $1,035\text{ cm}^{-1}$ was due to Si-O stretching frequency (Gunister et al. 2007). Figure 1b revealed the IR spectra of chitosan at $3,455\text{ cm}^{-1}$ was the O-H stretch. The peak at $2,867\text{ cm}^{-1}$ was typical C-H stretch. Pure chitosan has a peak absorbance at $1,561\text{ cm}^{-1}$, which corresponds to the N-H band for either primary amines or amide II (Osman and Arof 2003). The peak at $1,422\text{ cm}^{-1}$ corresponded to the CH_3 symmetrical deformation mode.

The intensity of $3,500\text{--}3,000\text{ cm}^{-1}$ reflected the stretching vibration of hydrogen bonding between the lattice hydroxyls and organic groups. It was stronger in pure chitosan film (Fig. 1b) compared to those incorporated with MMT (Fig. 1c) and PRP (Fig. 1d, e, and f). The characteristic peaks had shifted to lower frequencies in chitosan blend films which may be because some interaction between functional groups of chitosan, MMT and PRP (Abdollahi et al. 2012). As expected, all the characteristic peaks of chitosan were observed in FTIR spectra of the chitosan blend films. The peaks at $1,561\text{ cm}^{-1}$ (N-H band) and $1,422\text{ cm}^{-1}$ (C-H band), became sharper in the films incorporated with MMT. However, the peaks of these two strong water bands flattened more with incorporating PRP. This indicated that the group of N-H and C-H band reduced with increasing PRP concentration. The IR

spectra showed that PRP incorporation led to the presence of a new peak at $1,706\text{ cm}^{-1}$, that was only observed for chitosan films when PRP was added. The peak at $1,706\text{ cm}^{-1}$ which was corresponded to C=O stretching vibration increased with increasing PRP concentration. The result supported the assumption that there were interactions of PRP polyphenolic component with hydroxyl and amino groups in chitosan matrix.

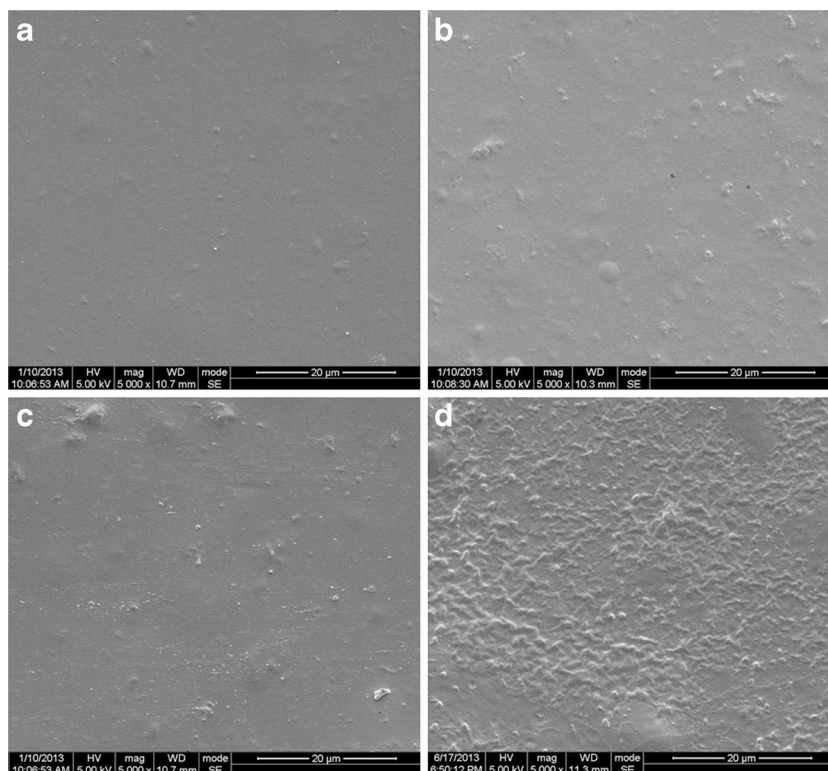
SEM analysis SEM micrographs of the surface morphology of pure chitosan, M1P1.5, M3P1.5, and M5P1.5 films (magnification: 5,000 \times) were shown in Fig. 2. The SEM investigations showed a homogenous dispersion of the components in the sample of pure chitosan (see Fig. 2a). However, in the chitosan-based composite films, the MMT particles were dispersed throughout the chitosan matrix, and a separation of chitosan matrix was observed (see Fig. 2b, c, and d).

Water Vapor Permeability (WVP) Since a main functional property of a food packaging is often to avoid or at least to decrease moisture transfer between the food and the surrounding atmosphere, WVP should be as low as possible (Gontard et al. 1992). The WVP values of the chitosan and chitosan-based composite films were shown in Table 1. As can be seen in Table 1, the water vapor barrier property of the films was significantly improved by incorporation of MMT and PRP ($p < 0.05$).

The WVP of pure chitosan film was found to be $2.18 \pm 0.02 \times 10^{-9}\text{ g}\cdot\text{m}/\text{m}^2\cdot\text{s}\cdot\text{Pa}$. There were 11.5 %, 13.8 %, and 20.6 % improvement in water vapor barrier properties at 1 %, 3 %, and 5 % of MMT in chitosan/MMT composites, respectively. This was probably due to the presence of ordered dispersed nanoparticle layers in the polymer matrix. This forced water vapor traveling through the film to follow a tortuous path through the polymer matrix surrounding the particles, and increased the effective path length for diffusion (Casariego et al. 2009; Rhim et al. 2006).

Additionally, the results indicated that an increase in PRP from 1 % to 2 % (w/w) decreased the WVP of chitosan/MMT-PRP composite films, whereas addition of 2 % (w/w) increased this property significantly ($p < 0.05$). For example, when the MMT loading was 3 %, addition of 1 %, 1.5 %, and 2 % of PRP in chitosan/MMT/PRP composites decreased the WVP values by 3.7 %, 8.5 %, and 13.3 %, respectively. When compared to pure chitosan film, the WVP of M3P2 film decreased by 25.2 %. The hydrogen and covalent interactions between chitosan network and polyphenolic compounds reduce the availability of the hydrophilic groups, subsequently lead to a decrease in the affinity of chitosan film towards water molecules (Siripatrawan and Harte 2010). The interactions between chitosan and PRP were also verified by FTIR spectrum.

Fig. 2 SEM micrographs of the surface morphology of **a** pure chitosan, **b** M1P1.5, **c** M3P1.5, and **d** M5P1.5 films (magnification: 5,000 \times). M1P1.5, M3P1.5, and M5P1.5-see Table 1



Mechanical properties The chitosan films incorporated MMT were prepared to improve the mechanical properties of the film. The thickness of the film containing MMT had a similar value among samples. However, it should be noted that the thickness of the chitosan/MMT-PRP composite film significantly ($p < 0.05$) increased with the addition of high molecular weight phenolic compounds in PRP. Although the film was prepared by the same amount of film-forming solution, the difference between samples was attributed to the different composition of film-forming solution (Lim et al. 2010).

Mechanical properties reflect the ability of film to protect the integrity of foods. Mechanical properties of the films were presented in Table 1. TS and E of pure chitosan film were 20.8 ± 1.2 MPa and 12.7 ± 0.8 %, respectively. The results showed that tensile strength (TS) of the films was affected by the addition of MMT. TS increased about 26 %, 60 %, and 55 % when the concentration of MMT was 1 %, 3 %, and 5 %, respectively. Elongation at break (E) of samples was also affected by incorporating MMT. When MMT was added into chitosan films alone, E increased about 25 %, 34 %, and 32 % when the concentration of MMT was 1 %, 3 %, and 5 %, respectively. The increase in TS or E of chitosan/MMT films may be due to the uniform dispersion of MMT in chitosan matrix and the strong interaction between chitosan and MMT (Xu et al. 2006).

When the concentration of PRP increased, TS was significantly improved ($p < 0.05$), even at a low amount of PRP. The

increase in TS mainly because the interactions between PRP polyphenolic component and chitosan matrix. To some extent, the increase of thickness also could improve the TS of blend films. However, percent elongation at break did not significantly ($p > 0.05$) changed by addition of PRP. This was probably because that the addition of PRP inside chitosan film induced the development of structural discontinuities (Martins et al. 2012).

Opacity of the films One of the desired characteristics of packaging material is that it should protect food from oxidative deterioration caused by visible and ultraviolet light. Table 2 showed the opacity of chitosan-based films incorporated with MMT and PRP. The transparency of chitosan/MMT films decreased significantly ($p < 0.05$) with increasing MMT content. This was similar to results to those of Rhim et al. (2006). The opacity values of chitosan films with PRP were significantly ($p < 0.05$) higher than those without PRP. A decrease in film transparent as a result of the addition of antioxidant had also been reported in gelatin-based films with oregano or rosemary extract (Gómez-Estaca et al. 2009).

Total phenolic content The total phenolic content of the chitosan-based films, evaluated by Folin–Ciocalteu method, was presented in Fig. 3. The phenolic contents can be used as an important indicator of antioxidant capacity and be used as a preliminary screen for any product when intended as antioxidants

Table 2 Opacity of the chitosan-based films

Film	T
Control	1.88±0.03 ^a
M1	2.62±0.20 ^{ab}
M1P1	4.46±0.28 ^{de}
M1P1.5	4.99±0.10 ^{de}
M1P2	5.54±0.47 ^e
M3	3.08±0.07 ^{bc}
M3P1	4.11±0.42 ^{cd}
M3P1.5	4.87±0.11 ^{de}
M3P2	4.85±1.13 ^{de}
M5	4.22±0.22 ^d
M5P1	4.41±0.28 ^{de}
M5P1.5	4.80±1.75 ^{de}
M5P2	4.51±0.13 ^{de}

*Values are given as mean ± standard deviation

Values followed by different letters in the same row are significantly different ($p < 0.05$), *a*=the lowest value

in food packing materials (Viuda-Martos et al. 2011). The results showed that total phenolic content of films significantly ($p < 0.05$) increased with increasing PRP concentration. The highest value (15.2 mg GAE/g DW) was for the film incorporated with 3 % MMT and 2 % PRP. Furthermore, the total phenolic content of films directly affected the antioxidant activity measured by DPPH radical-scavenging ability. Kanatt et al. (2012) reported that the incorporation of natural plant extract with high phenolic content, such as mint extract and pomegranate extract, in chitosan films enhanced antioxidant potential to the films. Mayachiew and Devahastin (2010) also indicated that the incorporation of gooseberry extract increased total phenolic content of chitosan films. However, the presence of MMT did not affect the total phenolic content and antioxidant ability of films. This might be because that MMT was an inorganic filler and it did not show antioxidant activity (Gutierrez et al. 2012).

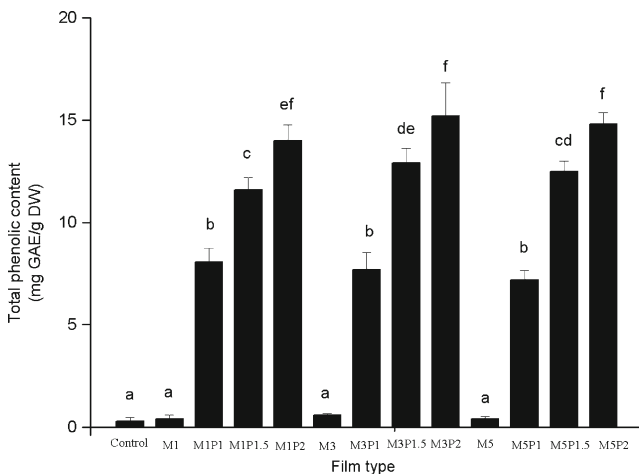


Fig. 3 The total phenolic content of the chitosan-based films. Results are mean ± standard deviation. Different letters indicate significantly different ($p < 0.05$), *a*=the lowest value

DPPH radical-scavenging ability The relatively stable organic radical, DPPH, has been widely used in the determination of antioxidant activity of single compounds, different plant extracts and film extracts. DPPH is a very stable organic free radical with deep violet color which gives absorption maxima within 515–528 nm range. Upon receiving proton from phenolics, it loses its chromophore and became yellow. The whole system allows a large number of samples to be tested in a short time (Arabshahi-Delouee and Urooj 2007).

DPPH radical-scavenging ability of the chitosan-based films was shown in Fig. 4. Pure chitosan films showed 3.03 % DPPH radical-scavenging ability, which might be because that the capacity of residual free amino groups of chitosan to react with free radicals forming stable macromolecular radicals and ammonium groups (Xie et al. 2001). The DPPH RSA significantly ($p < 0.05$) increased as PRP concentration increased. The film incorporated with 3 % MMT and 2 % PRP that contained the highest amount of total phenolic, was found to be the most active radical scavenger. The interaction between phenolic compounds and chitosan molecules could influence the DPPH radical-scavenging ability of the films. Similar trend had been reported by Siripatrawan and Harte (2010).

Conclusions

The present study showed that chitosan films can be made by incorporation of MMT and PRP. MMT could enhance water vapor permeability and mechanical properties of the chitosan-based films. FTIR spectra demonstrated that good interaction between functional groups of chitosan with MMT or with PRP. The compatibility of PRP with chitosan-MMT films

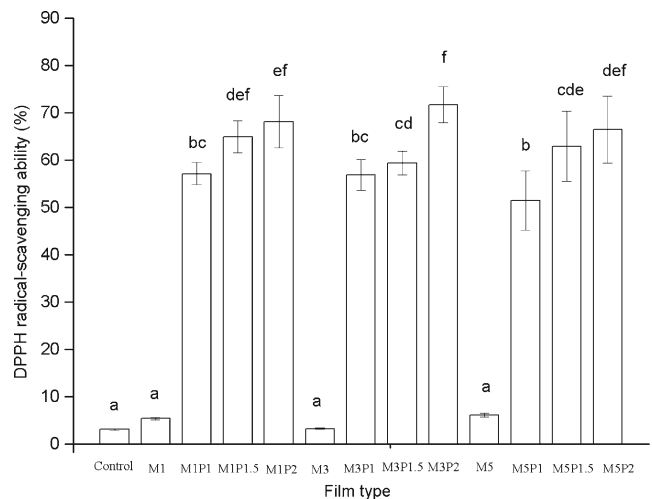


Fig. 4 The DPPH radical-scavenging ability of the chitosan-based films. Results are mean ± standard deviation. Different letters indicate significantly different ($p < 0.05$), *a*=the lowest value

was also confirmed. In addition, PRP extracts imparted excellent antioxidant activities to the films. Therefore, these films can be of great potential for being developed into functional packaging material for food and is a promising alternative to synthetic materials.

References

- Abdollahi M, Rezaei M, Farzi G (2012) A novel active bionanocomposite film incorporating rosemary essential oil and nanoclay into chitosan. *J Food Eng* 111:343–350
- Arabshahi-Delouee S, Urooj A (2007) Antioxidant properties of various solvent extracts of mulberry (*Morus indica* L.) leaves. *Food Chem* 102:1233–1240
- Avella M, De Vlioger JJ, Errico ME, Fischer S, Vacca P, Grazia VM (2005) Biodegradable starch/clay nanocomposite films for food packaging applications. *Food Chem* 93:467–474
- Casariogo A, Souza BWS, Cerqueira MA, Teixeira JA, Cruz L, Diaz R, Vicente AA (2009) Chitosan/clay films' properties as affected by biopolymer and clay micro/nanoparticles' concentrations. *Food Hydrocoll* 23:1895–1902
- Costa C, Conte A, Buonocore GG, Del Nobile MA (2011) Antimicrobial silver-montmorillonite nanoparticles to prolong the shelf life of fresh fruit salad. *Int J Food Microbiol* 148:164–167
- Devatkal SK, Naveena BM (2010) Effect of salt, kinnow and pomegranate fruit by-product powders on color and oxidative stability of raw ground goat meat during refrigerated storage. *Meat Sci* 85:306–311
- Devatkal SK, Narsaiah K, Borah A (2011) The effect of salt, extract of kinnow and pomegranate fruit by-products on colour and oxidative stability of raw chicken patties during refrigerated storage. *J Food Sci Technol* 48:472–477
- Gómez-Estaca J, Gómez-Guillén MC, Fernández-Martín F, Montero P (2011) Effects of gelatin origin, bovine-hide and tuna-skin, on the properties of compound gelatin-chitosan films. *Food Hydrocoll* 25:1461–1469
- Gómez-Estaca J, Montero P, Fernández-Martín F, Alemán A, Gómez-Guillén MC (2009) Physical and chemical properties of tuna-skin and bovine-hide gelatin films with added aqueous oregano and rosemary extracts. *Food Hydrocoll* 23:134–1341
- Gontard N, Guilbert S, Cuq JL (1992) Edible wheat gluten films: influence of the main process variables on film properties using response surface methodology. *J Food Sci* 57:190–195
- Guldás M, Akpınar-Bayzıt A, Özcan T, Yılmaz-Ersan L (2010) Effects of edible film coatings on shelf-life of mustafakemalpasasweet, a cheese based dessert. *J Food Sci Technol* 47:476–481
- Gunster E, Pestrel D, Unlu CH, Atıcı O, Gungor N (2007) Synthesis and characterization of chitosan-MMT biocomposite systems. *Carbohydr Polym* 67:358–365
- Gutierrez MQ, Echeverria I, Ihl M, Bifani V, Mauri AN (2012) Carboxymethylcellulose-montmorillonite nanocomposite films activated with murta (*Ugni molinae* Turcz) leaves extract. *Carbohydr Polym* 87:1495–1502
- Harris R, Lecumberri E, Mateos-Aparicio I, Mengibar M, Heras A (2011) Chitosan nanoparticles and microspheres for the encapsulation of natural antioxidants extracted from *Ilex paraguariensis*. *Carbohydr Polym* 84:803–806
- Hu Q, Fang Y, Yang Y, Ma N, Zhao L (2011) Effect of nanocomposite-based packaging on postharvest quality of ethylene-treated kiwifruit (*Actinidia deliciosa*) during cold storage. *Food Res Int* 44:1589–1596
- Huang B, He J, Ban X, Zeng H, Yao X, Wang Y (2011) Antioxidant activity of bovine and porcine meat treated with extracts from edible lotus (*Nelumbo nucifera*) rhizome knot and leaf. *Meat Sci* 87:46–53
- Jamshidian M, Tehrani EA, Imran M, Akhtar MJ, Cleymand F, Desobry S (2012) Structural, mechanical and barrier properties of active PLA-antioxidant films. *J Food Eng* 110:380–389
- Kanatt SR, Rao MS, Chawla SP, Sharma A (2012) Active chitosan-polyvinyl alcohol films with natural extracts. *Food Hydrocoll* 29:290–297
- Kumarasamy Y, Byres M, Cox PJ, Jaspars M, Nahar L, Sarker SD (2007) Screening seeds of some Scottish plants for free-radical scavenging activity. *Phytother Res* 21:615–621
- Lim GO, Jang SA, Song KB (2010) Physical and antimicrobial properties of Gelidium corneum/nano-clay composite film containing grapefruit seed extract or thymol. *J Food Eng* 98:415–420
- Martins JT, Cerqueira MA, Vicente AA (2012) Influence of α -tocopherol on physicochemical properties of chitosan-based films. *Food Hydrocoll* 27:220–227
- Mathew S, Abraham TE (2008) Characterisation of ferulic acid incorporated starch-chitosan blend films. *Food Hydrocoll* 22:826–835
- Mayachiew P, Devahastin S (2010) Effects of drying methods and conditions on release characteristics of edible chitosan films enriched with Indian gooseberry extract. *Food Chem* 118:594–601
- Moradi M, Tajik H, Rohani SMR, Oromiehie AR, Malekinejad H, Aliakbarlu J, Hadian M (2012) Characterization of antioxidant chitosan film incorporated with *Zataria multiflora* Boiss essential oil and grape seed extract. *LWT - Food Sci Technol* 46:477–484
- Naveena BM, Sen AR, Vaithyanathan S, Babji Y, Kondaiah N (2008) Comparative efficacy of pomegranate juice, pomegranate rind powder extract and BHT as antioxidants in cooked chicken patties. *Meat Sci* 80:1304–1308
- Negi PS, Jayaprakasha GK, Jena BS (2003) Antioxidant and antimutagenic activities of pomegranate peel extracts. *Food Chem* 80:393–397
- Osman Z, Arof AK (2003) FTIR studies of chitosan acetate based polymer electrolytes. *Electrochim Acta* 48:993–999
- Park P, Je J, Kim S (2004) Free radical scavenging activities of differently deacetylated chitosans using an ESR spectrometer. *Carbohydr Polym* 55:17–22
- Rhim JW (2006) The effect of clay concentration on mechanical and water barrier properties of chitosan-based nanocomposite films. *Food Sci Biotechnol* 15:925–930
- Rhim JW, Hong S, Park H, Perry KW (2006) Preparation and characterization of chitosan-based nanocomposite films with antimicrobial activity. *J Agr Food Chem* 54:5814–5822
- Selani MM, Contreras-Castillo CJ, Shirahigue LD, Gallo CR, Plata-Oviedo M, Montes-Villanueva ND (2011) Wine industry residues extracts as natural antioxidants in raw and cooked chicken meat during frozen storage. *Meat Sci* 88:397–403
- Seog EJ, Zuo L, Lee JH, Rhim JW (2008) Kinetics of Water Vapor Adsorption by Chitosan-based Nanocomposite Films. *Food Sci Biotechnol* 17:330–335
- Siripatrawan U, Harte B (2010) Physical properties and antioxidant activity of an active film from chitosan incorporated with green tea extract. *Food Hydrocoll* 24:770–775
- Takao T, Watanabe N, Yagi I, Sakata K (1994) A simple screening method for antioxidants and isolation of several antioxidants produced by marine bacteria from fish and shellfish. *Biosci Biotech Biochem* 58:1780–1783
- Vásconez MB, Flores SK, Campos CA, Alvarado J, Gerschenson LN (2009) Antimicrobial activity and physical properties of chitosan-tapioca starch based edible films and coatings. *Food Res Int* 42:762–769
- Viuda-Martos M, Ruiz-Navajas Y, Fernández-López J, Sendra E, Sayas-Barberá E, Pérez-Álvarez JA (2011) Antioxidant properties of

- pomegranate (*Punica granatum* L.) bagasses obtained as co-product in the juice extraction. Food Res Int 44:1217–1223
- Xie W, Xu P, Liu Q (2001) Antioxidant activity of water-soluble chitosan derivatives. Bioorg Med Chem Lett 11:1699–1701
- Xu YX, Kim KM, Hanna MA, Nag D (2005) Chitosan-starch composite film: preparation and characterization. Ind Crop Prod 21:185–192
- Xu YX, Ren X, Hanna MA (2006) Chitosan/clay nanocomposite film preparation and characterization. J Appl Polym Sci 99:1684–1691